Research Square

Preprints are preliminary reports that have not undergone peer review.
They should not be considered conclusive, used to inform clinical practice,
or referenced by the media as validated information.

Evaluation of the Relationship between Carcinoma-Associated Fibroblasts and Cancer Stem Cells in Oropharyngeal Squamous Cell Carcinoma

Mohamadreza Karimi
Tehran University of Medical Sciences
Motahareh Guneii
Tehran University of Medical Sciences
Farzad Yazdani
Tehran University of Medical Sciences
Mohammadreza Moeininejad
Tehran University of Medical Sciences
Abbas Karimi
Tehran University of Medical Sciences
Nazanin Mahdavi
Tehran University of Medical Science
Mohammad Javad Kharazi fard
Tehran University of Medical Sciences
Samira Derakhshan
sderakhshan@tums.ac.ir

Tehran University of Medical Science

Research Article

Keywords: Cancer-associated fibroblast, Cancer stem cell, Oropharyngeal squamous cell carcinoma, SOX10

Posted Date: August 10th, 2026

DOI: https://doi.org/10.21203/rs.3.rs-10322540/v1

License: This work is licensed under a Creative Commons Attribution 4.0 International License.
Read Full License

Additional Declarations: No competing interests reported.

Abstract

Aim

Cancer-associated fibroblasts (CAFs) and cancer stem cells (CSCs) contribute to tumor aggressiveness. We evaluated the correlation between SOX10 (CSC marker) and CAFs in HPV-related and non-HPV-related oropharyngeal squamous cell carcinoma (OPSCC) and their possible association with microRNAs.

Methods

Thirty-one OPSCC paraffin blocks were analyzed using SOX10 and α-SMA immunohistochemistry. HPV presence was determined by nested PCR. Expression of miR-221, miR-222, and miR-155 was assessed by real-time PCR. Statistical analyses were performed ($p \leq 0.05$ considered significant).

Results

Most cases showed high SOX10 expression. No correlation was found between SOX10 and α-SMA scores, but SOX10 was associated with a shorter time to relapse. HPV status showed no relation to SOX10, though its association with α-SMA was nearly significant. miR-221 and miR-222 were upregulated, while miR-155 was downregulated, but none correlated significantly with SOX10 or CAFs.

Conclusion

The lack of correlation between SOX10 and α-SMA suggests SOX10 does not influence CAFs. However, elevated SOX10 expression may shorten relapse time. These findings offer insights into CSC characteristics in OPSCC and their potential association with CAFs.

Introduction

Oropharyngeal squamous cell carcinoma (OPSCC) is a significant subtype of head and neck cancer, with its incidence rising globally, partly due to the increasing prevalence of human papillomavirus (HPV)-associated cases. HPV-positive OPSCCs tend to exhibit better survival outcomes and a more favorable clinical course compared to their HPV-negative counterparts (1).

The tumor microenvironment (TME) plays a pivotal role in cancer progression, with cancer-associated fibroblasts (CAFs) and cancer stem cells (CSCs) emerging as critical contributors to tumor aggressiveness and therapeutic resistance (2). The TME consists of non-malignant cells surrounding the bulk of the tumor. CAFs are one of the important components of this area. These cells interact with cancerous cells and other constituents of the TME to support tumor progression. They have the capacity

to induce local invasiveness, angiogenesis, and metastasis. They are typically characterized by α-smooth muscle actin (α-SMA) expression (3, 4).

Another influential component of the TME is cancer stem cells (CSCs), which drive tumor initiation, metastasis, and relapse due to their capacities for self-renewal, differentiation, and resistance to therapy (5, 6). These tumor-initiating cells have been shown to resist conventional treatments such as chemotherapy and contribute to stemness-related features that promote recurrence and metastatic potential (7, 8).

MicroRNAs (miRNAs) are a group of single-stranded, endogenously synthesized RNAs that do not code for proteins. It has been shown that miRNAs exhibit altered expression profiles in tumoral lesions compared to normal tissues (9). There is a strong association between deregulated miRNA expression and tumor growth, distorted cellular processes, unregulated proliferation, and the self-renewal capacity of CSCs in various cancers, including those of the head and neck (9, 10).

In OPSCC, the interplay between CAFs and CSCs remains poorly understood, particularly in the context of HPV status, which significantly influences disease prognosis and treatment response. The current study aims to investigate the relationship between SOX10 expression, as a marker of CSCs, and the presence of CAFs (identified by α-SMA expression) in HPV-related and non-HPV-related OPSCC. Furthermore, we explore the correlation between these factors and the expression of miR-221, miR-222, and miR-155. Understanding these interactions may shed light on mechanisms of tumor aggressiveness and identify new prognostic biomarkers or therapeutic targets in OPSCC.

Method and Material

Patients and Samples

A total of 31 formalin-fixed paraffin-embedded (FFPE) tissue samples diagnosed with primary OPSCC were obtained from Amir Alam and Shariati hospitals, affiliated with Tehran University of Medical Sciences. Inclusion criteria comprised: (1) histologically confirmed primary OPSCC, (2) surgical treatment with tumor resection, (3) no history of chemotherapy or radiotherapy before surgery, and (4) availability of archived FFPE tissue blocks. Demographic and clinical information, including age, sex, diagnosis date, recurrence, and treatment data, was collected from patients' medical records. This study was conducted as part of two undergraduate theses supported by the School of Dentistry, Tehran University of Medical Sciences (grants #1400-2-133-53411 and #1400-3-133-56066), and was approved by the university's Ethics Committee (IR.TUMS.DENTISTRY.REC.1400.107 and IR.TUMS.DENTISTRY.REC.1401.011).

Histology and Immunohistochemical assay

Tumor grading was performed using the 2017 WHO classification of head and neck tumors, categorizing samples as low, intermediate, or high grade(11). Inflammatory cell infiltration was assessed in eight hot spot fields around tumor nests using an Olympus BX-51 microscope at ×400 magnification. The level of infiltration was scored as mild (< 500 cells), moderate (500–1000 cells), or severe (> 1000 cells).

All 31 OPSCC tissue blocks were cut into 4 μm thick sections. For immunohistochemical detection of α-SMA (used for CAF assessment), slides were deparaffinized and incubated with a monoclonal mouse anti-human smooth muscle actin antibody (Dako, Clone 1A4, Code M0851, dilution 1:100). The procedure utilized Dako Antibody Diluent (Code S0809) and the streptavidin-biotin peroxidase complex system, processed using the Ventana Benchmark automated stainer. Negative controls were prepared by omitting the primary antibody and using phosphate-buffered saline, based on a previously established protocol (4).

SOX10 staining was conducted using a rabbit monoclonal anti-human SOX-10 antibody (Clone EP268, Master Diagnostica, Spain; dilution 1:50), following the manufacturer's instructions. Malignant melanoma tissue was used as a positive control.

Sections were mounted on charged slides and dried overnight at 60°C. Slides were then deparaffinized, rehydrated, and subjected to heat-induced epitope retrieval (HIER) using citrate buffer (pH 6.4) at 95°C for 20 minutes in the Pt Module. Slides were rinsed several times with distilled water and cooled to room temperature for 20 minutes. Endogenous peroxidase was blocked for 10 minutes at room temperature (Ref. MAD-021540Q-125). Slides were then incubated with the primary antibody (1:50) for 10 minutes. The Master Polymer Plus Detection System (HRP, DAB included; Ref. MAD-000237QK) was used for visualization, followed by hematoxylin counterstaining and mounting.

Immunohistochemical analysis

Each stained section was independently reviewed by two trained oral pathologists, who performed blinded evaluations for all markers. All slides were assessed under a light microscope (Olympus BX-51, Japan). For α-SMA, cytoplasmic staining in non-inflammatory, non-endothelial spindle-shaped stromal cells was interpreted as positive, with blood vessel walls serving as internal positive controls. CAF expression was evaluated based on both staining intensity and the proportion of positive cells. The assessment followed a four-point scale adapted from Lin (12). Intensity scores were assigned as follows: 0 (no staining at ×400 magnification), 1 (staining detectable only at ×400), 2 (visible at ×100 but not ×40), and 3 (clearly visible at ×40).

The proportion of immunopositive cells was graded as: 0 (< 1%), 1 (≥ 1% to < 33%), 2 (≥ 33% to < 66%), and 3 (≥ 66%). The final immunostaining score was calculated by multiplying the intensity and proportion scores. Based on this combined score, samples were categorized as: negative (score 0), weakly positive (scores 1–2), moderately positive (scores 3–4), or strongly positive (scores 6–9) (12).

For SOX10, positive staining was defined as nuclear localization in tumor cells. The scoring method was based on the four-tiered system reported by Adams and Kang (13, 14), with the following categories: Strong (3+), characterized by intense staining visible at low magnification involving > 50% of cells; Moderate (2+), either focal intense staining in < 50% of cells or moderate staining in > 50% of cells; Weak (1+), pale or focal moderate staining involving < 50% of tumor cells and not prominent at low power; and Negative (0+), with no staining observed.

Quantitative real-time PCR

Total RNA extraction

Total RNA was extracted following the manufacturer's protocol, which involved five primary steps: homogenization, phase separation, precipitation, washing, and reconstitution. Sections (10 µm) from FFPE samples were first snap-frozen in liquid nitrogen, then ground into fine powder using a mortar and pestle. Approximately 50–100 mg of powdered tissue was homogenized in 1 mL of YTzol reagent (YTzol Pure RNA, Cat. No: YT9066, Yekta Tajhiz Azma, Iran) using a rotor-stator homogenizer.

For phase separation, samples were incubated at room temperature for 5 minutes to allow dissociation of nucleoprotein complexes. Then, 0.2 mL of chloroform was added per 1 mL of reagent, tubes were sealed and vigorously shaken for 15 seconds, followed by incubation for 2–3 minutes and centrifugation at 12,000 × g for 5–10 minutes at 4°C. This step resulted in a biphasic separation: the upper aqueous phase containing RNA, an interphase, and a lower phenol-chloroform phase. The aqueous layer, approximately 60% of the original reagent volume, was carefully transferred to a fresh tube.

RNA was precipitated by adding 0.5 mL of isopropanol per 1 mL of reagent and mixing by inversion. After 10 minutes of incubation at 15–30°C, the mixture was centrifuged again at 12,000 × g for 5–10 minutes at 4°C. A gel-like pellet formed at the tube's base. The pellet was washed twice with 1 mL of 75% ethanol, gently inverted, centrifuged (12,000 × g, 2 min, 4°C), and ethanol was discarded. The RNA pellet was then vacuum-dried for 5–10 minutes and redissolved in 0.5% SDS by pipetting and heating at 55–60°C for 10 minutes. Finally, RNA was resuspended in 100% formamide and stored at − 70°C. Only samples with A260/280 ratios below 1.6 were used for downstream applications.

cDNA synthesis

Complementary DNAs (cDNAs) corresponding to mature miRNAs—miR-221-3p, miR-222, and miR-155—were synthesized from 300 ng of total RNA using the ExcelRT™ Reverse Transcription Kit (SMOBIO, RP1300, RXN100, Taiwan). The primer sequences used in the reverse transcription reactions were as follows:

miR-221-3p:

Stem: GTCGTATCCAGTGCAGGGTCCGAGGTATTCGCACTGGATACGACGAAACC

Forward: CGTGAGGAGCTACATTGTCTGC

miR-222-3p:

Stem: GTCGTATCCAGTGCAGGGTCCGAGGTATTCGCACTGGATACGACACCCAG

Forward: CGTTGGAGCTACATCTGGC

miR-155-5p:

Stem: GTCGTATCCAGTGCAGGGTCCGAGGTATTCGCACTGGATACGACAACCCC

Forward: GGCTGGTTAATGCTAATCGTGA

U6 (internal control):

Stem: GTCGTATCCAGTGCAGGGTCCGAGGTATTCGCACTGGATACGACAAAATATGG

Forward: GCAAGGATGACACGCAAATTC

For denaturation, a mixture containing 2 μg RNA, 1 μg primers, and 6–7 μL of DEPC-treated water was incubated at 70°C for 5 minutes and immediately cooled on ice for 1 minute. A reverse transcription mixture consisting of 4 μL 5× RT buffer (DTT), 4 μL DEPC-treated water, 1 μL RNAok™ RNase Inhibitor, and 1 μL ExcelRT™ Reverse Transcriptase was added. The reaction was incubated at 25°C for 10 minutes, followed by enzyme inactivation at 85°C for 5 minutes and then cooled to 4°C. RNase H (1 μL) was then added and incubated at 37°C for 20 minutes to degrade RNA templates. The resulting cDNA was stored at − 20°C or used immediately for real-time PCR.

PCR method

Quantitative real-time PCR was carried out using the RealQ Plus 2× Master Mix Green (AMPLIQON, Cat. No. A325402) on an ABI StepOnePlus™ system, following the manufacturer's protocol. Each 15 μL reaction consisted of 25 ng cDNA, 1 μL of forward primer, a variable volume of PCR-grade water, and 12.5 μL of the 2× master mix.

Thermal cycling conditions were as follows: an initial denaturation at 95°C for 15 minutes, followed by 40 amplification cycles of 95°C for 15 seconds and 60°C for 1 minute. All samples were analyzed in triplicate. The expression of miR-221, miR-222, and miR-155 was quantified using the comparative Ct (ΔΔCt) method and normalized to the U6 small RNA reference gene.

Nested PCR

Genomic DNA was extracted from FFPE tissue punches using the DNA FFPE Tissue Kit (GeneAll, Korea), following the manufacturer's instructions, as previously described [1]. HPV detection was performed using a nested PCR (nPCR) approach with universal primers capable of identifying HPV genotypes 6, 11, 16, 18, 30, 31, 33, 39, 52, 53, 54, 58, 59, 61, 66, and 68.

External primers MY09 (5′-CGTCCMARRGGAWACTGATC-3′) and MY11 (5′-GCMCAGGGWCATAAYAATGG-3′) were employed in the first PCR round. Internal amplification was then carried out using GP5+ (5′-TTTGTTACTGTGGTAGATACTAC-3′) and GP6+ (5′-GAAAAATAAACTGTAAATCATATTC-3′) primers.

Amplification was conducted using a Bio-Rad T100 thermal cycler with the following cycling parameters: initial denaturation at 95°C for 5 minutes; 40 cycles at 95°C for 1 minute, 56°C for 1 minute (external primers) or 52°C for 30 seconds (internal primers), and 72°C for 1 minute; followed by a final extension at 72°C for 10 minutes.

PCR products were analyzed on 1% agarose gel via electrophoresis. Fluorescent bands were visualized using a gel documentation system. Reactions were validated with house-keeping primers serving as internal controls.

Statistical analysis

Statistical analyses were performed using IBM SPSS software, version 22.0. Due to the potential non-normal distribution of variables, the Mann–Whitney U test was used to compare SOX10 and α-SMA expression between HPV-positive and HPV-negative groups. Spearman's rank correlation coefficient was applied to assess associations between these markers.

The relationships between SOX10 expression levels and clinicopathologic variables were analyzed using either the Kruskal–Wallis or Mann–Whitney U test, depending on the number of groups. Associations between CAF scoring and miRNA expression profiles were examined using the Chi-square (χ^2) test. A p-value ≤ 0.05 was considered statistically significant.

Results

Demographic/histopathologic information and HPV

This study included 31 patients with oropharyngeal squamous cell carcinoma (OPSCC), of whom 16 were HPV-positive and 15 were HPV-negative. Among the participants, 28 (90.7%) were male and 3 (9.7%) were female. Ages ranged from 46 to 87 years, with a mean age of 61 years.

In the HPV-positive group, 8.7% were female, compared to 4.8% in the HPV-negative group (p = 0.605). The mean age was 62.78 years (SD = 10.471; range: 46–87) in HPV-positive patients and 60.95 years (SD = 9.759; range: 48–83) in the HPV-negative group, with no significant difference between groups (p = 0.565).

Regarding histologic grade, the HPV-positive group included 7 high-grade, 3 intermediate-grade, and 6

low-grade tumors. The HPV-negative group included 9 intermediate-grade and 6 low-grade tumors; no high-grade tumors were observed. There was no statistically significant association between tumor grade and HPV status.

Inflammatory infiltrate intensity was also evaluated. Among HPV-positive cases, 7 had severe, 6 had moderate, and 3 had mild inflammation. In the HPV-negative group, 9 cases had severe, 2 had moderate, and 4 had mild inflammation. No significant association was found between inflammation severity and HPV status (Table 1).

SOX10 and α-SMA immunohistochemistry

SOX10 immunohistochemical staining revealed 10 cases with a score of +1, 13 with +2, and 7 with+3.Only one case was negative (score 0) (Figure 1).

The mean SOX10 score was 1.69 (SD = 0.873; range: 0–3) in HPV-positive cases and 2.00 (SD = 0.756; range: 1–3) in HPV-negative cases. This difference was not statistically significant (Table 2).

The mean α-SMA score was 2.44 (SD = 0.727; range: 1–3) in the HPV-positive group and 1.73 (SD = 1.223; range: 0–3) in the HPV-negative group. **The difference approached statistical significance (p = 0.06).**

Spearman's correlation analysis showed no significant correlation between SOX10 and α-SMA scores (r = 0.159, p = 0.393) (Table 3).

Mirs evaluation

Melt curves and acrylamide gel electrophoresis confirmed successful amplification of target miRNAs (Figures 2 and 3). The results showed miR-221 and miR-222 were significantly upregulated and miR-155 was downregulated in OPSCC samples. There was no significant correlation between miRs expression and HPV status (p-value greater than 0.05). In 29 cases of high expression of miR-221 and miR-222, 13 showed score 3 and 9 showed score 2 for α-SMA and only 4 cases showed no expression for α-SMA (Table 4 and 5). In all 31 cases of low expression of miR-155, 14 showed score 3 and 10 showed score 2 for α-SMA. 4 cases showed no expression and 3 cases showed score 1 for α-SMA (Table 6). These results showed that upregulation of miR-221 and miR-222 and downregulation of mir-155 in tumoral cells may be correlated with increased in CAFs in OPSCC. However, no significant relation was found between these miRs expression and CAFs (p-value greater than 0.05).

Relapse

The follow-up period was assessed from the time of diagnosis, according to pathology reports, until the last contact with the patient or the most recent clinical examination in uncertain cases. For deceased patients, follow-up was recorded from the date of diagnosis to the date of death. The follow-up duration ranged from 1 to 87 months.

Regarding the relationship between relapse and HPV status, SOX10 score, and α-SMA score, the results showed that relapse or death occurred in 64.3% of HPV-positive patients and 63.6% of HPV-negative

patients (p = 0.648). There was no significant correlation between miRNA expression and relapse status (p > 0.05).

As shown in Table 7, the mean SOX10 score in patients with relapse was 1.63 (SD = 0.885; range: 0–3), whereas in patients without relapse, it was 2.23 (SD = 0.667; range: 0–3). In patients who experienced relapse, the mean α-SMA score was 2.00 (SD = 1.033; range: 0–3), compared to 2.22 (SD = 1.000; range: 0–3) in those without relapse (Table 7).

We also evaluated the association between time to relapse and both SOX10 and α-SMA scores. The analysis demonstrated that an increase in SOX10 score was significantly associated with a shorter time to relapse (p < 0.05). However, there was no significant relationship between time to relapse and α-SMA score (p = 0.781) (Table 7). Additionally, no significant correlation was observed between miRNA expression and time to relapse (p > 0.05).

Discussion

This study investigated the relationship between cancer-associated fibroblasts (CAFs), cancer stem cells (CSCs), and selected microRNAs (miR-155, miR-221, and miR-222) in oropharyngeal squamous cell carcinoma (OPSCC), with a particular focus on differences related to HPV status and their clinical implications. Our most significant finding was that increased expression of SOX10, a recognized CSC marker, was associated with a shorter time to relapse in OPSCC patients. This observation supports the hypothesis that CSC-related features contribute to more aggressive tumor behavior and early disease recurrence in this subset of head and neck cancer.

Cancer stem cells (CSCs), characterized by self-renewal capacity and tumor-initiating potential, are typically identified by surface or nuclear markers such as SOX2, SOX10, OCT3/4, ALDH1, CD44 and CD133 and etc (15). SOX10, a member of the big known SOX family, acts as a transcription factor for differentiation, migration and also maintenance of several tissues which are derived from neural crest cells (16). However, some studies have provided evidences of SOX10 expression in the salivary gland, breast, and ovarian neoplasms affecting epithelial cells (17). In nasopharyngeal carcinomas, substantial overexpression of SOX10 was observed. In addition, higher expression of SOX10 was associated with poorer prognosis. It showed that SOX10 may be involved in tumor growth and metastasis in nasopharyngeal carcinoma (16–18). These findings are in line with our results, as we evaluated and reported that increased SOX10 scores were associated with a shorter time to relapse in OPSCC, suggesting that SOX10 may serve as a prognostic biomarker in clinical practice.

In parallel, we assessed cancer-associated fibroblasts (CAFs) presence via α-smooth muscle actin (α-SMA) immunohistochemistry. CAFs, known for their high potential to enhance tumor aggressiveness, are frequently observed in the tumor microenvironment (TME) of high-grade HPV-positive OPSCCs (4). Some studies have reported that CAFs secrete cytokines, enzymes, and various proteins that exert functional effects on head and neck tumor cells (19, 20). Moreover, CAFs have been shown to promote stemness in oral cancer cells(21). For instance, Patel et al. demonstrated that a subtype of CAFs with high α-SMA

expression increases self-renewal and ALDH1 expression (as a CSC marker) in oral cancer cells more than CAFs with low α-SMA expression. Interestingly, CAFs with lower α-SMA expression may suppress stemness through BMP4 signaling (21).

While α-SMA scores were higher in HPV-positive tumors, consistent with prior reports (4), we did not observe a statistically significant correlation between SOX10 and α-SMA scores. This finding suggests that while CAFs are frequently present in OPSCC, their association with CSC prevalence may be more complex than previously thought. Shi et al. demonstrated that cancer-associated fibroblasts (CAFs) are key architects of the tumor microenvironment, promoting cancer stem cell (CSC) survival and expansion in lung metastases of squamous cell carcinoma by providing a TGF-β-mediated CSC niche (22). Parajuli climbed a-SMA expression at tumor front but not in center of tumor has prognostic value for survival in head and neck squamous cell carcinoma (23). Spatial heterogeneity within the tumor, such as differences between the invasive front and tumor core, may influence CAF–CSC interactions, but our sample design did not account for this, representing a study limitation.

Analysis of miRNA expression revealed consistent upregulation of miR-221 and miR-222 and downregulation of miR-155 in OPSCC samples, but no statistically significant associations were found between these miRNAs and either SOX10 or α-SMA expression. Notably, these expression trends align with their established oncogenic and tumor-suppressive functions in cancer biology For instance, miR-221 and miR-222 have been shown to promote proliferation, migration, and resistance to apoptosis in oral squamous cell carcinoma by targeting tumor suppressors such as CDKN1B (24, 25). Similarly, miR-155 downregulation has been associated with impaired immune modulation and more aggressive tumor phenotypes in head and neck cancers (26, 27). Although our data did not confirm a direct relationship between these miRNAs and CSC or CAF markers in OPSCC, it is possible that their effects are mediated through indirect pathways or require a larger sample size to achieve statistical power.

The absence of significant correlations between CAFs, CSCs, and miRNA expression in this study may also be influenced by sample size limitations, inter-patient biological variability, and the use of immunohistochemical scoring without spatial profiling. Moreover, while we used ΔCt values to define high and low miRNA expression, future studies incorporating quantitative thresholds validated by functional assays and protein-level confirmation will enable a more realistic association.

Conclusion

In conclusion, our findings suggest that SOX10 expression may serve as a prognostic indicator of early relapse in OPSCC. Although the roles of CAFs and selected miRNAs remain less clearly defined in this context, observed expression trends warrant further investigation. Future research with larger cohorts, spatial tumor profiling, and integrated transcriptomic analysis will be critical to fully elucidate the interplay between CSCs, CAFs, and miRNA-driven regulatory networks in OPSCC progression.

Declarations

Ethics approval and consent to participate

Ethical approval of this study was obtained from the Ethics Committee of Tehran University of Medical Sciences and Health Services (Approval No. IR.TUMS.DENTISTRY.REC.1400.107 and IR.TUMS.DENTISTRY.REC.1401.011).

Consent to participate

The requirement for written informed consent was waived by the Ethics Committee of Tehran University of Medical Sciences because this study was conducted on archived formalin-fixed tissue samples long after patients' diagnosis and treatment, with no direct patient contact and no additional intervention.

Declaration of Helsinki

The study was conducted in accordance with the Declaration of Helsinki and relevant national guidelines.

Consent to publish

Not applicable.

Conflict of interest

There is no conflict of interest for authors who were involved in this research.

Funding

This research has been supported and granted by Tehran University of Medical Sciences and Health Services, School of Dentistry in grant numbers #1400-2-133-53411 and #1400-3-133-56066.

Author Contribution

M. Karimi and M. Guneii contributed equally to the conceptualization and the first draft of the manuscript. A. Karimi, F. Yazdani and M. Moeininejad were responsible for the methodology. M. J. Kharazi Fard and N. Mahdavi performed the data investigation and formal analysis. S. Derakhshan assisted in the validation and review process. S. Derakhshan provided supervision, resources, and final editing. All authors contributed to the final revision of the article.

Acknowledgment

The authors would like to thank Tehran University of Medical Sciences and Health Services, School of Dentistry, for its support of this research.

Data Availability

The datasets generated and analyzed during the current study are available from the corresponding author on reasonable request.

References

1. Lechner M, Liu J, Masterson L, Fenton TR. HPV-associated oropharyngeal cancer: epidemiology, molecular biology and clinical management. Nat reviews Clin Oncol. 2022;19(5):306–27.
2. Quail DF, Joyce JA. Microenvironmental regulation of tumor progression and metastasis. Nat Med. 2013;19(11):1423–37.
3. Sahai E, Astsaturov I, Cukierman E, DeNardo DG, Egeblad M, Evans RM, et al. A framework for advancing our understanding of cancer-associated fibroblasts. Nat Rev Cancer. 2020;20(3):174–86.
4. Rahrotaban S, Mahdavi N, Abdollahi A, Yazdani F, Kaghazloo A, Derakhshan S. Carcinoma-associated fibroblasts are a common finding in the microenvironment of HPV-positive Oropharyngeal squamous cell carcinoma. Appl Immunohistochem Mol Morphology. 2019;27(9):683–8.
5. Batlle E, Clevers H. Cancer stem cells revisited. Nat Med. 2017;23(10):1124–34.
6. Curtarelli RB, Gonçalves JM, Dos Santos LGP, Savi MG, Nör JE, Mezzomo LAM, et al. Expression of cancer stem cell biomarkers in human head and neck carcinomas: a systematic review. Stem cell reviews Rep. 2018;14:769–84.
7. Najafi M, Farhood B, Mortezaee K. Cancer stem cells (CSCs) in cancer progression and therapy. J Cell Physiol. 2019;234(6):8381–95.
8. Chang JC. Cancer stem cells: Role in tumor growth, recurrence, metastasis, and treatment resistance. Medicine. 2016;95(1S):S20–5.
9. Barlak N, Capik O, Sanli F, Karatas OF. The roles of microRNAs in the stemness of oral cancer cells. Oral Oncol. 2020;109:104950.
10. Khan AQ, Ahmed EI, Elareer NR, Junejo K, Steinhoff M, Uddin S. Role of miRNA-regulated cancer stem cells in the pathogenesis of human malignancies. Cells. 2019;8(8):840.
11. El-Naggar AK, Chan JK, Rubin Grandis J, Slootweg PJ. WHO classification of head and neck tumours. (No Title). 2017.
12. Lin NN, Wang P, Zhao D, Zhang FJ, Yang K, Chen R. Significance of oral cancer-associated fibroblasts in angiogenesis, lymphangiogenesis, and tumor invasion in oral squamous cell carcinoma. J Oral Pathol Med. 2017;46(1):21–30.

13. Adams E, Green J, Clark A, Youngson J. Comparison of different scoring systems for immunohistochemical staining. J Clin Pathol. 1999;52(1):75–7.
14. Kang Y, Pekmezci M, Folpe AL, Ersen A, Horvai AE. Diagnostic utility of SOX10 to distinguish malignant peripheral nerve sheath tumor from synovial sarcoma, including intraneural synovial sarcoma. Mod Pathol. 2014;27(1):55–61.
15. Gunduz M, Gunduz E, Tamagawa S, Enomoto K, Hotomi M. Cancer stem cells in oropharyngeal cancer. Cancers. 2021;13(15):3878.
16. Bahmad HF, Thiravialingam A, Sriganeshan K, Gonzalez J, Alvarez V, Ocejo S, et al. Clinical significance of SOX10 expression in human pathology. Curr Issues Mol Biol. 2023;45(12):10131–58.
17. Lee JH, Kang HJ, Yoo CW, Park WS, Ryu JS, Jung Y-S, et al. PLAG1, SOX10, and Myb expression in benign and malignant salivary gland neoplasms. J Pathol Translational Med. 2019;53(1):23–30.
18. Zhao Y, Liu Z-g, Tang J, Zou R-f, Chen X-y, Jiang G-m et al. High expression of Sox10 correlates with tumor aggressiveness and poor prognosis in human nasopharyngeal carcinoma. OncoTargets therapy. 2016:1671–7.
19. Custódio M, Biddle A, Tavassoli M. Portrait of a CAF: The story of cancer-associated fibroblasts in head and neck cancer. Oral Oncol. 2020;110:104972.
20. Kumar D, New J, Vishwakarma V, Joshi R, Enders J, Lin F, et al. Cancer-associated fibroblasts drive glycolysis in a targetable signaling loop implicated in head and neck squamous cell carcinoma progression. Cancer Res. 2018;78(14):3769–82.
21. Patel AK, Vipparthi K, Thatikonda V, Arun I, Bhattacharjee S, Sharan R, et al. A subtype of cancer-associated fibroblasts with lower expression of alpha-smooth muscle actin suppresses stemness through BMP4 in oral carcinoma. Oncogenesis. 2018;7(10):78.
22. Shi X, Luo J, Weigel KJ, Hall SC, Du D, Wu F, et al. Cancer-associated fibroblasts facilitate squamous cell carcinoma lung metastasis in mice by providing TGFβ-mediated cancer stem cell niche. Front Cell Dev Biology. 2021;9:668164.
23. Parajuli H, Teh MT, Abrahamsen S, Christoffersen I, Neppelberg E, Lybak S, et al. Integrin α11 is overexpressed by tumour stroma of head and neck squamous cell carcinoma and correlates positively with alpha smooth muscle actin expression. J Oral Pathol Med. 2017;46(4):267–75.
24. Chen Q, Wang W, Wang Y. MiR-222 regulates the progression of oral squamous cell carcinoma by targeting CDKN1B. Am J Translational Res. 2022;14(7):5215.
25. Lamirel C, Newman NJ, Biousse V. Vascular neuro-ophthalmology. Neurol Clin. 2010;28(3):701–27.
26. Hess A-K, Müer A, Mairinger FD, Weichert W, Stenzinger A, Hummel M, et al. MiR-200b and miR-155 as predictive biomarkers for the efficacy of chemoradiation in locally advanced head and neck squamous cell carcinoma. Eur J Cancer. 2017;77:3–12.
27. Liu X, Liu P, Chernock RD, Yang Z, Lang Kuhs KA, Lewis JS Jr, et al. A MicroRNA expression signature as prognostic marker for oropharyngeal squamous cell carcinoma. JNCI: J Natl Cancer Inst. 2021;113(6):752–9.

Tables

Tables are available in the Supplementary Files section.

Figures

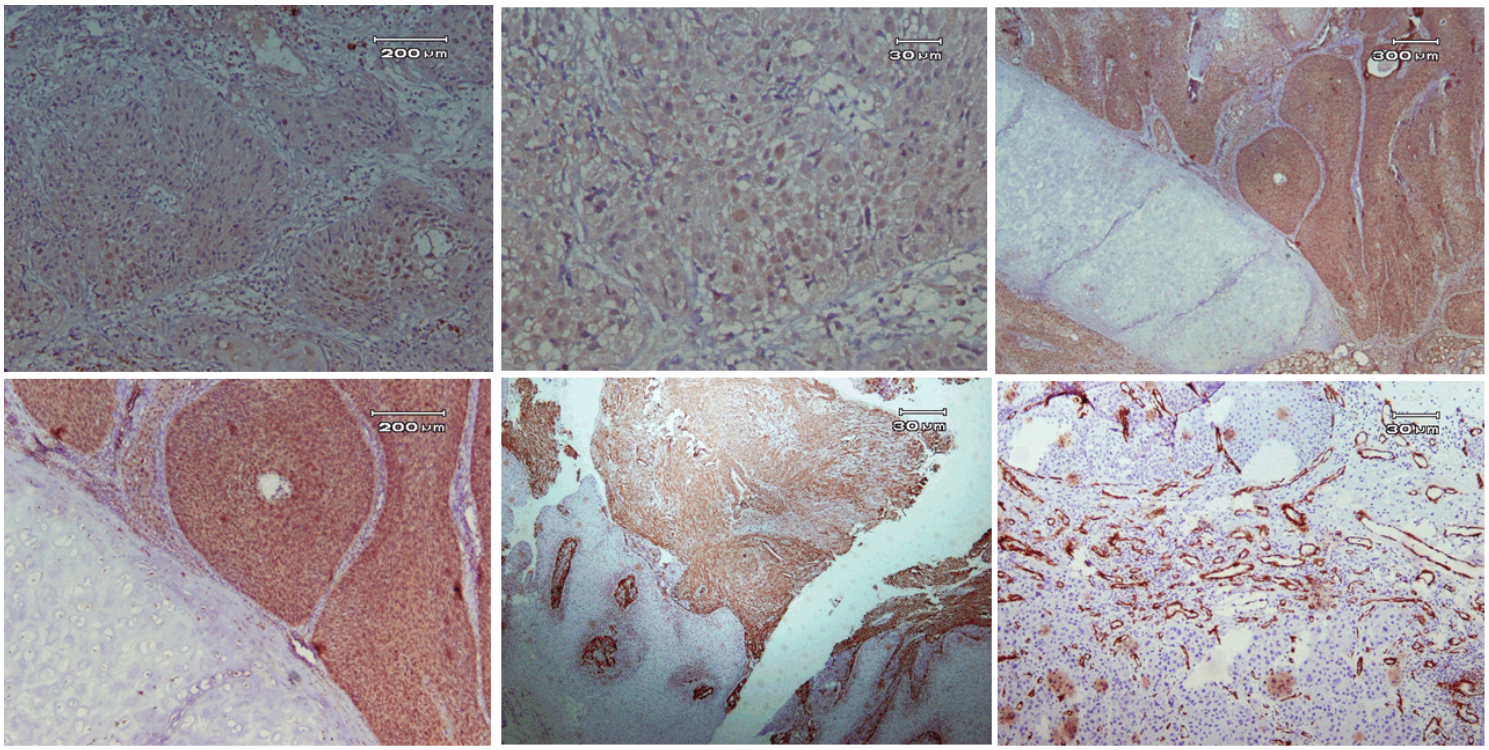


Figure 1

IHC staining. a-Weak nuclear staining (score +1) of SOX10 marker (×200 magnification, up/left). b-Weak nuclear staining (score +1) of SOX10 marker (×400 magnification, up/mid). c-Strong nuclear staining (score +3) of SOX10 marker (×100 magnification, up/right). d- Strong nuclear staining (score +3) of SOX10 marker (×200 magnification, down/left). e-Score 3 of immunostaining for α-SMA (proportion of positive cells more than 66%) in stromal cells (×100 magnification, down/mid). f- Positive immunoreactivity for α-SMA in stromal blood vessels as internal positive control (×400 magnification, down/right).

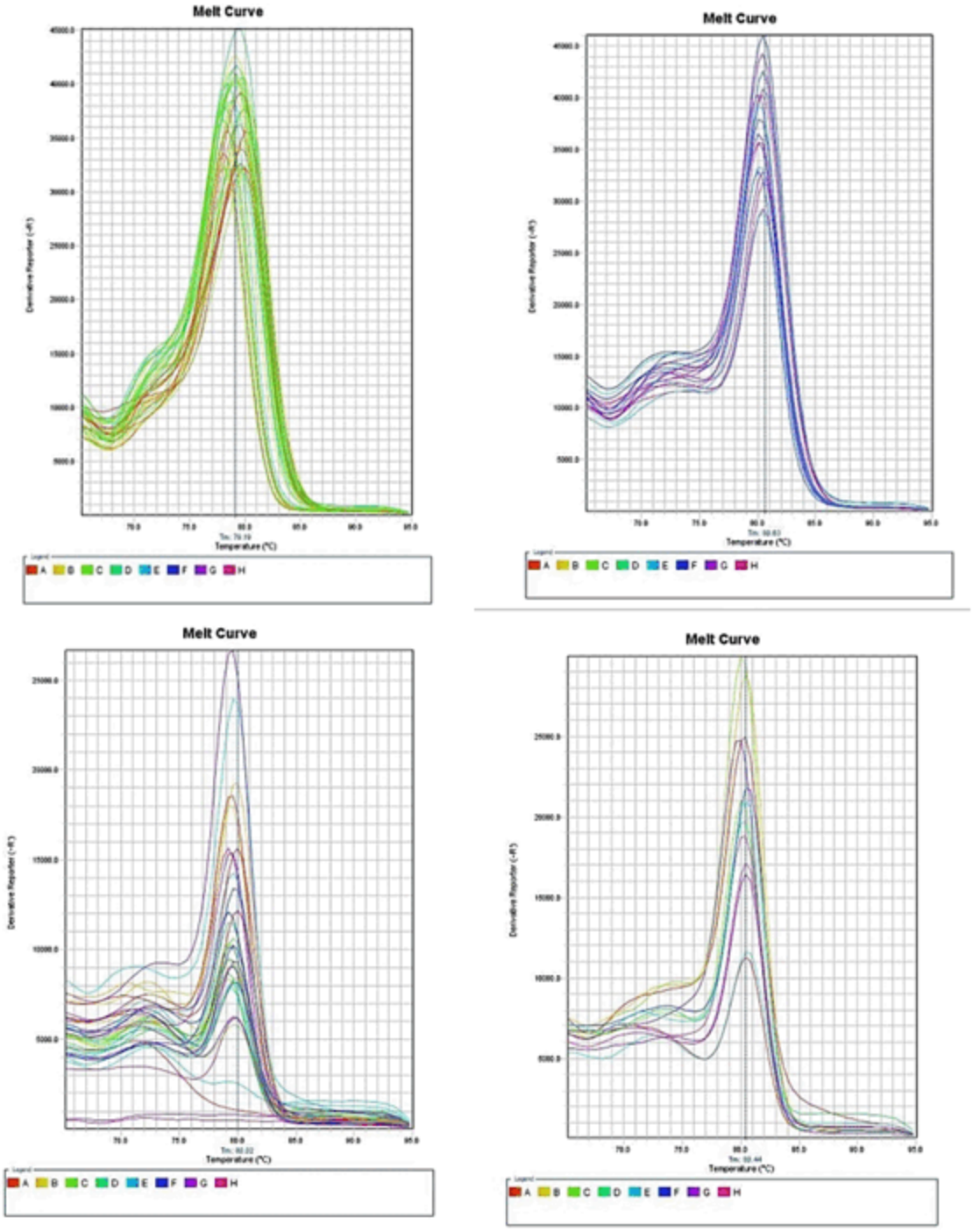


Figure 2

Melting curves for miR-221, miR-222, miR-155, and U6, respectively.

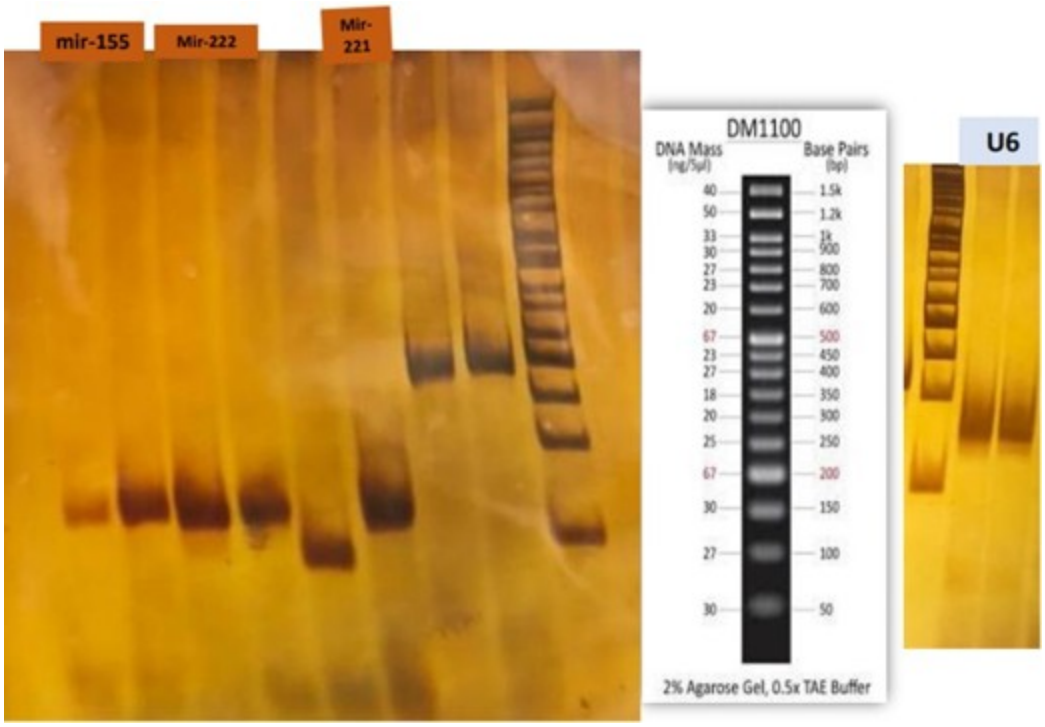


Figure 3

Acrylamide gel confirmed pairs of miR-155, miR-222, miR-221, and U6 genes in 74, 71, 76, and 74 bands, respectively.

Supplementary Files

This is a list of supplementary files associated with this preprint. Click to download.

- Tables2.docx